Preliminary experimental and numerical studies of light-core vortex rings

Thien Duy Nguyen*, Nolan Goth*, Pablo Moresco+, Vincent Jodoin+, Vivek Rao*

*Nuclear Energy and Fuel Cycle Division, Oak Ridge National Laboratory, Oak Ridge, TN, USA
+Nuclear Nonproliferation Division, Oak Ridge National Laboratory, Oak Ridge, TN, USA
nguyend@ornl.gov, gothne@ornl.gov, morescopd@ornl.gov, jodoinvj@ornl.gov, raovm@ornl.gov
doi.org/10.13182/T130-44592

INTRODUCTION

Vortex rings are central to the description of numerous fluid flows, ranging from the formation of cumulus clouds in meteorology [1], macroscopic descriptions of liquid helium [2], and building elements in models of turbulence [3]. They are also crucial to many industrial applications, especially the transport of heat and mass [4]. In the ideal case, vortex rings can be described as an axisymmetric distribution of azimuthal vorticity, the *core*, which propagates, carrying with it a mass of irrotational fluid, called its *bubble* or *atmosphere*. When the core has a lower density than the surrounding fluid, it creates a buoyant vortex ring [5], which is a common occurrence following the introduction of a localized density perturbation in a relatively short period of time. Typical examples of vortex rings are thermals in the atmosphere [6] and the clouds formed as a result of explosions [7]. Vortex rings grow in radius as they propagate, resulting in the entrainment of surrounding fluid, the increase in the mass of the bubble, and a reduction in the velocity of propagation. This is related to viscous effects, fluctuations in the core vorticity, and buoyancy [8]. For buoyant vortex rings, the entrainment rate is orders of magnitude larger than nonbuoyant case [5], which has a substantial influence on the evolution of these vortices, especially in stratified flows, and on their ability to induce transport and enhance mixing [9]. Differences in density between the core and its atmosphere also affect the stability of the ring, its transition to a turbulent state, and its life span and eventual disintegration [10]. For practical reasons, most experimental studies of buoyant vortex rings have focused on small density differences [11] apart from studies of vortex bubbles, where more than one phase is present [12]. It is possible to adapt motion-equations for slightly buoyant rings [13], but few experimental/analytical results exist for the case of strongly buoyant vortex rings.

This paper summarizes our efforts on experimental and numerical studies of light-core vortex rings with a density ratio of 7.4 between the ring and ambient gas. The work focuses on the development of an experimental facility for the study of rings with very light cores in miscible fluids to better characterize the dependence of the vortex properties on the formation process, its transition to different stability regimes, and its relation to the stratification of the surrounding fluid. These data will be a valuable source of information for the understanding of the underlying physical processes and developing and future models of these types of flows. These models are used, for example, in the transport and dispersion of pollutants as part of routine industrial processing and emergency response activities [14].

DESCRIPTIONS OF EXPERIMENTAL STUDY

Figure 1 illustrates the transparent test facility designed to study buoyant vortex rings generated by the sudden release of a light gas in an environment containing heavy gas featuring nonintrusive flow visualization techniques. The current study employed the helium–nitrogen gas pair (density ratio of ρ_{Ni}/ρ_{He}=7.4) at an atmospheric pressure associated with 850 ft above sea level and at a temperature of 21°C. The light gas–filled soap bubbles were successfully tested and applied as the light gas release method. A 3 mm tube and compression nut with a bore diameter of 12.7 mm was used as the injection nozzle to create the helium bubbles, whose diameters are approximately 25.4 mm. Immediately after the burst of the bubble's surface, the internal volume of helium gas would begin to rise because of the density difference with the surrounding heavy gas. Consequently, the vortex ring formed and evolved as it continued to rise. In this study, sequential images of the filling process, bubble-burst event, and evolution of the buoyant vortex ring evolution were taken at 200 frames per second (fps) with a resolution of 2,560 × 1,600 pixels. The test facility was flushed after five vortex rings had been generated.

Background-oriented Schlieren Technique

The background-oriented Schlieren (BOS) technique was applied to qualitatively characterize the evolution of the buoyant vortex ring in the test facility. The experimental setup is illustrated in Figure 1*(a)*, including a high-speed Phantom VEO 440 camera capable of taking photos at 1,100 Hz at a resolution of 2,560 × 1,600 pixels, background panels of randomly generated dots positioned behind the test facility, and high-power LED lights (15,000 lm output) to illuminate the background pattern. A LaVision's PTUX synchronizer was used to temporally align the trigger timing sequences of the camera and light source. BOS is an optical density visualization technique that applies a digital image correlation approach on a background pattern to qualitatively and quantitatively characterize thermal fluid flow behaviors [15]. The BOS technique is based on the relation between the refractive index of a fluid (liquid/gas) and its density, given by the Lorentz–Lorenz equation, which can be simplified to the Gladstone–Dale equation for gaseous media [15]. In other

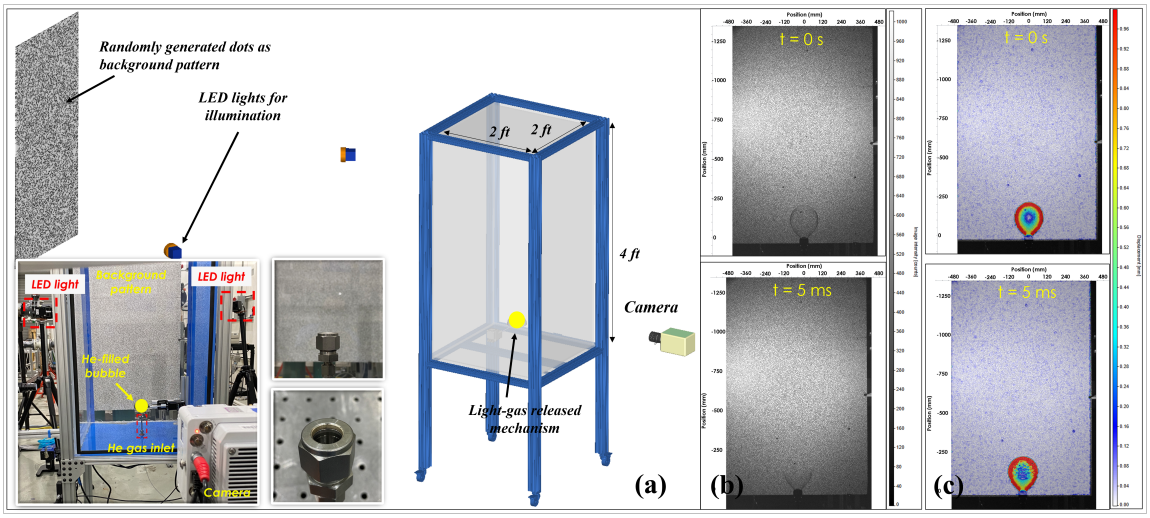

Fig. 1: *(a)* Experimental facility of buoyant vortex ring alongside the computer-aided design. *(b)* Raw BOS images highlighting a helium-filled bubble and background dot patterns. *(c)* Computed displacements caused by the difference in refractive index between the two gases.

words, BOS technique could indirectly determine physical properties, such as temperature, density, and other that are wavelength-dependent, by tracking the change of refractive index integrated along the line of sight between a camera and a static background pattern. An advantage of BOS is the simplicity of the setup and the robustness of the correlation-based analysis, making it useful and applicable to a wide variety of compressible and incompressible flows. A sensitivity study of BOS background images to measured results is discussed in [16]. A reference image of the background pattern with no density difference was captured and later used to evaluate images of regions of interest with a density difference (shown in Figure 1*([b])*) using the cross-correlation algorithm developed and optimized for the (PIV) technique.

Experimental results

Figure 1*(b–c)* illustrates raw BOS images and results of the displacement of the background dot patterns caused by the difference between the refractive index of the two gases to visualize the motion of the light gas and vortex ring evolution. Figure 2*(a)* is an image series following the breakdown of the bubble and shows the helium gas volume immediately migrating in the vertical direction because of the buoyant force. The nearly spherical volume transitioned to a mushroom shape at the distance of approximately two bubble diameters from the nozzle. Additionally, a counter-rotating vortex core was observed inside the cloud. The size and shape of the vortex core was found to change as the ring evolves. As the vortex ring moved along the vertical direction, smaller features detached, leaving a trail of elongated structures. The ability to quantitatively obtain the velocity of vortex ring structures is crucial to understanding the cloud evolution process for various initial conditions. Figure 2, *(b)* illustrates the maximum normal strain (depicted as a grayscale scalar contour) extracted from the displacement fields shown in *(a)*. An overlaid vector field depicts the velocity of the extracted features using PIV postprocessing algorithms. Results in Figure 2 show the vortex ring evolution is buoyant because the primary motion of the light gas cloud is in the opposite direction of gravity. The maximum velocity of the extracted features from the vortex ring was approximately 2 m/s.

DESCRIPTIONS OF NUMERICAL STUDY

Figure 3 presents the computational domain and generated mesh of the vortex ring study with a symmetrical boundary condition applied to reduce computational costs. This size is acceptable for all gas pairs and can accommodate up to 100 mm diameter cups or bubbles without the introduction of wall effects on the buoyant flow. The fluid-flow physics were modeled using a segregated flow with the implicit unsteady Reynolds-averaged Navier–Stokes $k-\omega$ shear-stress transport turbulence model [17] and low y^+ wall treatment. In the $k-\omega$ shear-stress transport model, a second-order convection scheme was applied. The volume of fluid (VOF) multiphase model [18] was chosen to simulate and identify the interface between light and heavy gases. The second-order convection scheme was implemented along with high-resolution interface capturing options to accurately resolve the interfaces between the two gases. The second-order temporal discretization was selected, and a time step of 0.005 s was chosen for the simulation period. The interaction length scale model was applied with a primary and secondary regime of 1.587 mm and 0.158 mm, respectively. The mixture multiphase model was used to calculate the interaction between the light and heavy gases. This model can be used for an arbitrary combination of phases with any phase interaction. Furthermore, if the mixture of phases can accurately represent the quantities of the individual phases, the mixture multiphase model can be used as an alternative to the more expensive Eulerian multiphase simulations. Mesh generation was performed using the automatic

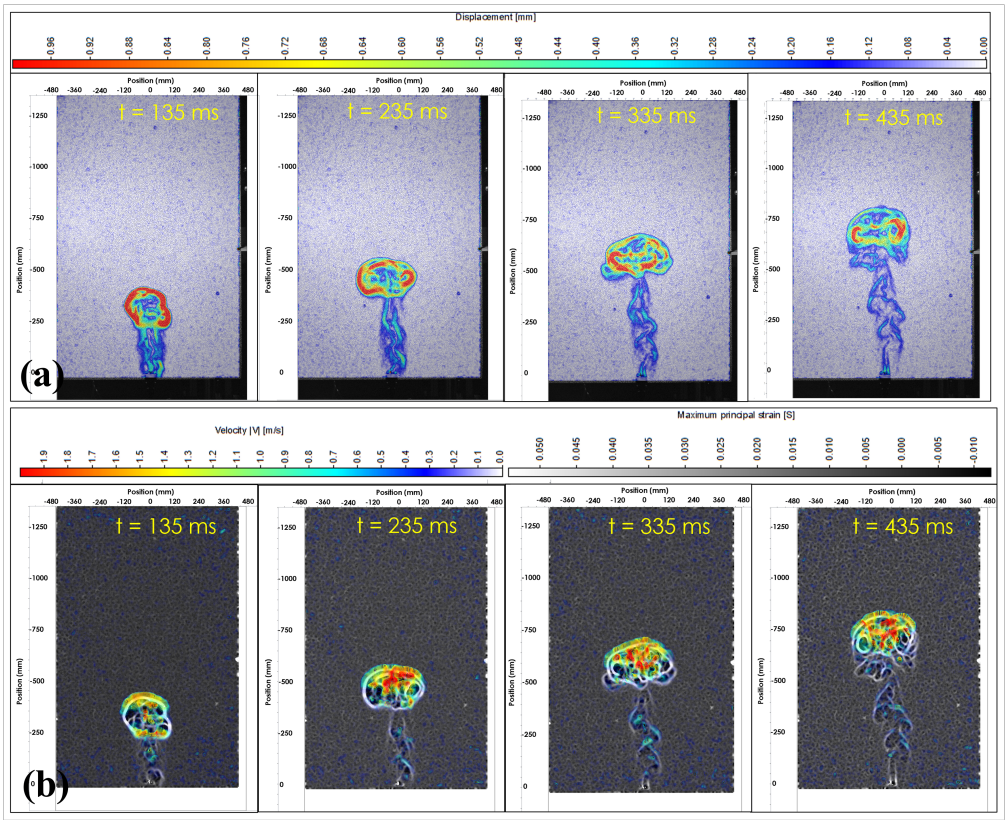

Fig. 2: *(a)* Color contour indicates displacements of background patterns caused by the evolution of a buoyant vortex ring. *(b)* Grayscale contour displays maximum normal strain computed from the displacements, and the colored vectors illustrate the velocity magnitude of the extracted normal strain feature computed using PIV algorithms.

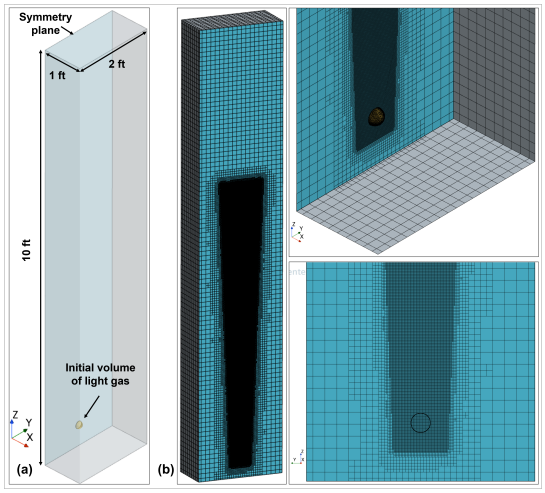

Fig. 3: Computer simulations of a vortex ring. *(a)* Computational domain. *(b)* Generated mesh.

structured octree meshing capability in Star-CCM+. The surface remesher, trimmed cell mesher, and prism layer mesher were used. Figure 4 illustrates the computational fluid dynamics (CFD) results of a buoyant vortex ring. In this calculation, the light gas (helium) volume was initiated as a 50 mm diameter sphere in a heavy gas (nitrogen). Images of the vorticity isosurfaces at different time intervals reveal the formation of a vortex ring and its evolution. Spatial structures of vortex rings obtained from the simulations reveal the shapes and sizes of a spherical volume transitioning to a mushroom-shaped bubble while rising, which is also observed in the BOS results. The CFD results also depict the counter-rotating vortex core inside the bubble cloud and finer features creating a trail of elongated structures. The size and rise velocity of the vortex ring from the BOS results shown in Figure 2 are in a satisfactory agreement with the CFD results displayed in Figure 4, i.e., ~1.5–2 m/s. The the BOS results, however, show that the overall structures of the vortex ring are not perfectly symmetrical. This could be associated to air disturbances that occurred in the test section during the experiments. Further comparisons between experiments and CFD will be supported using additional comprehensive instrumentation and measurement techniques.

CONCLUSIONS

This report summarizes the development of an experimental test facility to produce measurements for the advancement and validation of numerical models of the transport and dispersion of pollutant releases. The facility supports buoyant vortex

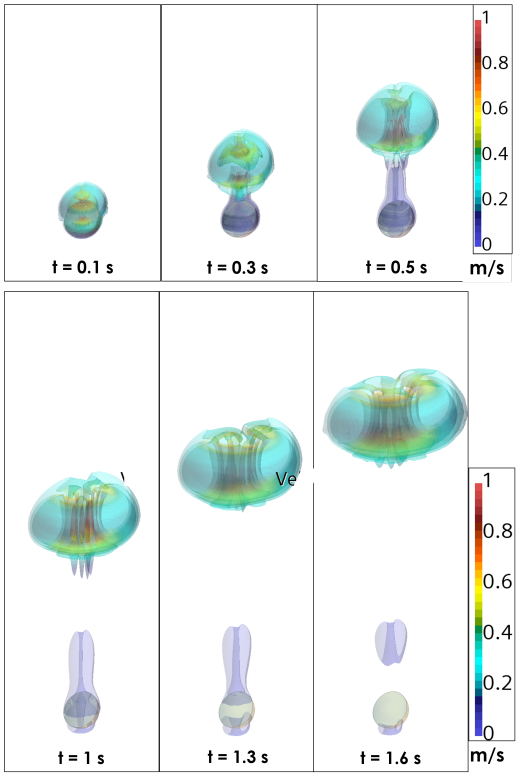

Fig. 4: Buoyant vortex ring from a CFD solution of vorticity magnitude (Ω) isosurfaces $\Omega = 3$ s^{-1}, 9 s^{-1}, and 21 s^{-1} from t = 0.1 to t = 1.6. The light gas (helium) volume was initialized as a 50 mm diameter sphere inside a heavy gas (nitrogen). Color contours show velocity magnitude (m/s).

rings with density ratios between the environment and the ring core ranging from 7 to 67 and encompassing relevant regimes. In addition, 3D CFD simulations using the URANS-VOF approach were performed to support the experimental design as well as provide insight about the formation and evolution of a vortex ring. The BOS technique has been successfully applied to buoyant vortex rings generated from the burst of helium-filled bubbles, while the laser diagnostic technique of PIV can be used in future studies to obtain the velocity field of the cloud and ring evolution. Results obtained from the URANS-VOF simulations illustrated the evolution and transitions of the flow structures associated to the vortex ring. Plans for future work include measurements of mixing phenomena of light and heavy gases and the combination of PIV or BOS and laser-induced fluorescence techniques. More complex volumetric measurements of velocity and density can be achieved using stereoscopic (2D three-component) and tomographic (3D three-component) PIV or BOS systems. Numerical simulations utilizing subgrid-scale-resolved large-eddy simulation (LES) turbulence modeling would enable the resolution of finer-scale coherent structures within the cloud and vortex ring flow evolution. This may prove beneficial for capturing entrainment r phenomena and predicting the stabilization height of the vortex ring.

ACKNOWLEDGEMENTS

This work was funded by the Department of Energy's National Nuclear Security Administration, Office of Defense Nuclear Nonproliferation Research and Development.

REFERENCES

1. J. LEVINE, "Experiments on convection of isolated masses of buoyant fluid," *J. Meteor.*, **16**, 653–662 (1959).
2. R. J. DONNELLY, "Quantized Vortices and Turbulence in Helium II," *Annu. Rev. Fluid Mech.*, **25**, 325–371 (1993).
3. P. G. SAFFMAN, "Vortex Models of Isotropic Turbulence," *Phil. Trans. R. Soc. Lond. A*, **355**, 1949–1956 (1997).
4. H. H. JABBAR and A. M. NAGUIB, "A computational study of vortex rings interacting with a constant-temperature heated wall," *Int. J. Heat Fluid Flow*, **76**, 197–214 (2019).
5. J. S. TURNER, "Buoyant vortex rings," *Proc. Roy. Soc. A*, **239**, 61–75 (1957).
6. B. MCKIM, N. JEEVANJEE, and D. LECOANET, "Buoyancy-driven entrainment in dry thermals," *Q. J. R. Meteorol. Soc.*, **146**, 415–425 (2020).
7. O. G. SUTTON, "The atom bomb trial as an experiment in convection," *Weather*, **2**, 105–110 (1947).
8. K. SHARIFF and A. LEONARD, "Vortex rings," *Annu. Rev. Fluid Mech.*, **24**, 235–279 (1992).
9. J. S. TURNER, "Turbulent entrainment: the development of the entrainment assumption, and its application to geophysical flows," *J. Fluid Mech.*, **173**, 431–471 (1986).
10. T. MAXWORTHY, "Some experimental studies of vortex rings," *J. Fluid Mech.*, **81**, 465–495 (1977).
11. R. S. SCORER, "Experiments on convection of isolated masses of buoyant fluid," *J. Fluid Mech.*, **2**, 583–594 (1957).
12. J. K. WALTERS and J. F. DAVIDSON, "The initial motion of a gas bubble formed in an inviscid liquid. Part 2. The three-dimensional bubble and the toroidal bubble," *J. Fluid Mech.*, **17**, 321–336 (1963).
13. E. A. SPIEGEL and G. VERONIS, "On the Boussinesq approximation for a compressible fluid," *Asprophys. J.*, **131**, 442–447 (1959).
14. H. G. NORMENT and S. WOOLF, "Department of Defense Land Fallout Prediction System. Volume III. Cloud Rise (Revised)," Report DASA-1800-III, Defense Atomic Support Agency (1970).
15. M. RAFFEL, "Background-oriented schlieren (BOS) techniques," *Experiments in Fluids*, **56**, *3*, 1–17 (2015).
16. F. REICHENZER, M. SCHNEIDER, and A. HERKOMMER, "Improvement in systematic error in background-oriented schlieren results by using dynamic backgrounds," *Experiments in Fluids*, **62**, 1–18 (2021).
17. F. R. MENTER, "Two-equation eddy-viscosity turbulence models for engineering applications," *AIAA Journal*, **32**, *8*, 1598–1605 (1994).
18. C. W. HIRT and B. D. NICHOLS, "Volume of fluid (VOF) method for the dynamics of free boundaries," *Journal of Computational Physics*, **39**, *1*, 201–225 (1981).